infrastructures

MDPI

Article

Fatigue Consideration for Tension Flange over Intermediate Support in Skewed Continuous Steel I-Girder Bridges

Dariya Tabiatnejad [1,*], Seyed Saman Khedmatgozar Dolati [1,*], Armin Mehrabi [1] and Todd A. Helwig [2]

[1] Department of Civil and Environmental Engineering, Florida International University, Miami, FL 33174, USA; amehrabi@fiu.edu
[2] Department of Civil, Architectural and Environmental Engineering, University of Texas at Austin, Austin, TX 78758, USA; thelwig@mail.utexas.edu
* Correspondence: dtabi003@fiu.edu (D.T.); skhed004@fiu.edu (S.S.K.D.)

Abstract: Skewed supports complicate load paths in continuous steel I-girder bridges, causing secondary stresses and differential deformations. For a continuous bridge where tensile stresses are developed in the top flange of the steel girders over the intermediate supports, these effects may exacerbate potential fatigue issues for the top flanges. There is a gap in knowledge regarding the level of stress one can expect at these locations, and the stress level can render the problem either serious or trivial. This paper has been successful in providing this information, which was not available before. The study examines the fatigue performance of the top flange in girders over skewed supports. Results are presented from a detailed investigation consisting of 3D finite element modeling to evaluate 26 skewed bridges in the State of Florida that represent the wide range of geometries found in practice. The analysis focused on stress ranges in the top flanges and axial demands on end cross-frame members under fatigue truck loading. A preliminary analysis helped to select the appropriate element type and support conditions. The maximum factored stress range of 3.63 ksi obtained for the selected group of bridges remains below the 10 ksi fatigue threshold for an AASHTO Category C connection, alleviating the concerns about the fatigue performance of the continuous girder top flange over the intermediate pier. Hence, fatigue is unlikely to be a concern in the flanges at this location. Statistics on computed stress ranges and cross-frame forces that provide an understanding of the expected values and guidance for detailing practices are also presented. A limited comparative refined FE analysis on two different types of end cross-frame to girder connections also provided useful insight into the fatigue sensitivities of the skew connections. Half-Round Bearing Stiffener (HRBS) connections performed better than the customary bent plate connections. The HRBS connection reduces girder flange stress concentration range by at least 18% compared to the bent plate connection. The maximum stress concentration range in bent plate components is significantly higher than in the HRBS connection components. The work documented in this paper is important for understanding the fatigue performance of the cross-frames and girders in support regions in the upcoming 10th edition of the AASHTO Bridge Design Specifications that may include plate stiffeners oriented either normally or skewed to the girder web, or Half-Round Bearing Stiffeners.

Keywords: skewed bridges; steel I-girder bridges; fatigue analysis; finite element analysis; end cross-frames

check for updates

Citation: Tabiatnejad, D.; Khedmatgozar Dolati, S.S.; Mehrabi, A.; Helwig, T.A. Fatigue Consideration for Tension Flange over Intermediate Support in Skewed Continuous Steel I-Girder Bridges. *Infrastructures* **2024**, *9*, 99. https://doi.org/10.3390/infrastructures9070099

Academic Editor: Marco Bonopera

Received: 11 April 2024
Revised: 13 June 2024
Accepted: 13 June 2024
Published: 26 June 2024

Copyright: © 2024 by the authors. Licensee MDPI, Basel, Switzerland. This article is an open access article distributed under the terms and conditions of the Creative Commons Attribution (CC BY) license (https://creativecommons.org/licenses/by/4.0/).

1. Introduction

According to the Federal Highway Administration (FHWA) report in 2022 [1], the United States boasts 619,622 bridges, many of which are skewed bridges. Support skew is a measure of the orientation of the longitudinal axis of the bridge relative to the line of the abutment or pier supports. Normal or right bridges have a perpendicular line of supports relative to the longitudinal axis of the bridge. However, due to geometrical

constraints, intersecting roads, and local terrain, the line of supports often must be offset by a skew angle—the angle between the bridge's end supports and a line perpendicular to its longitudinal axis (Figure 1). This definition aligns with the skew angle description provided by the AASHTO LRFD [2].

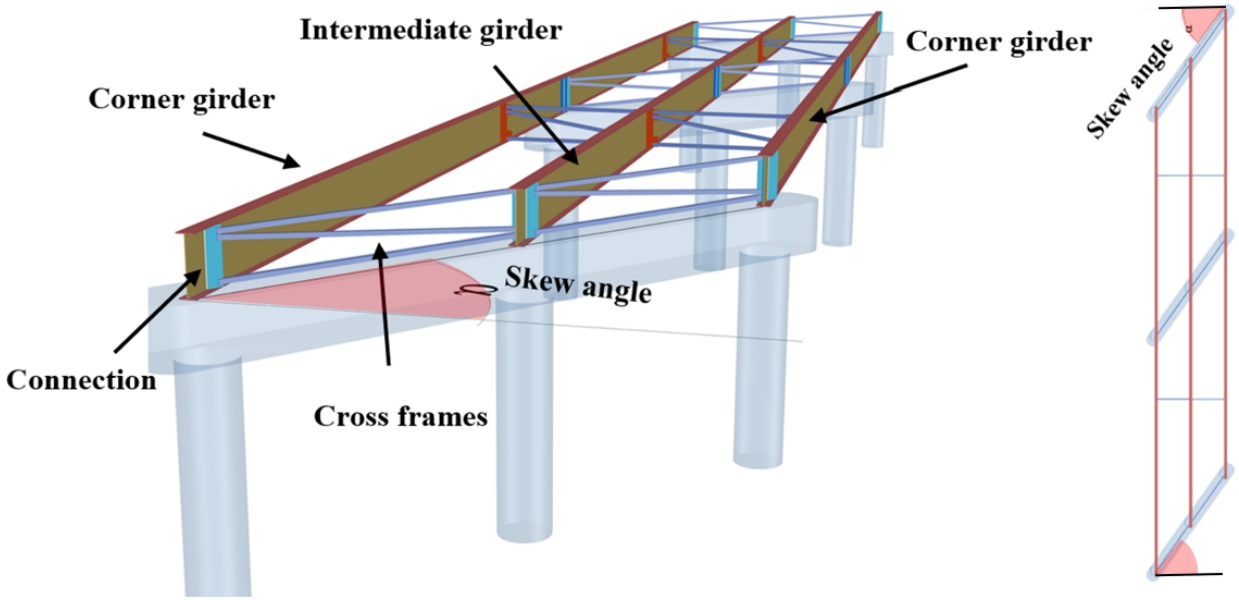


Figure 1. A skew angle in a steel I-girder bridge under construction before casting concrete deck.

Figure 1 illustrates a skewed steel girder bridge, showing structural elements such as steel I-girders, cross-frames, and piers. The design of skewed bridges demands careful consideration due to their unique structural behavior, which significantly differs from that of bridges with normal supports [3,4]. The skewness affects the force transfer within the girders and cross-frames, altering their interaction and leading to increased live load-induced stresses.

The force flow in skewed bridge decks is complex. The unique force distribution in girders with skewed supports often results in out-of-plane distortions and secondary stresses in the steel elements, particularly at skewed corners where maximum support reactions typically occur [5]. In bridges with skew angles larger than 20 degrees, AASHTO requires that intermediate cross-frames be oriented perpendicular to the longitudinal axis of the girders. Larger skew angles result in significant differences between the vertical deformations at the two ends of a cross-frame, intensifying the interaction between the cross-frames and girders, which increases the potential for fatigue in both the braces and the girders, as noted by Wang [6].

It is understood that fatigue becomes a concern for an element under tension that experiences stress variation. One major fatigue concern at the connection is the distortional fatigue that increases the joint sensitivity to the fatigue. Distortion effects can occur at the skewed end cross-frame connection regardless of whether the span is continuous or not. An example of a distortion-induced fatigue crack is shown in Figure 2. In addition to distortional fatigue, there is another mechanism involving the stiffeners welded to the girder flange in tension and/or constraint against flange bending, which has the potential to initiate fatigue cracks in the flange. An example of a fatigue-prone zone at the connection of the stiffener to the girder flange is shown in Figure 3. It should also be noted that this paper focuses on the specific skewed connection of the cross-frame to the girder and does not include fatigue mechanisms in other locations, e.g., deck/diaphragm under the effect of wheel loading.

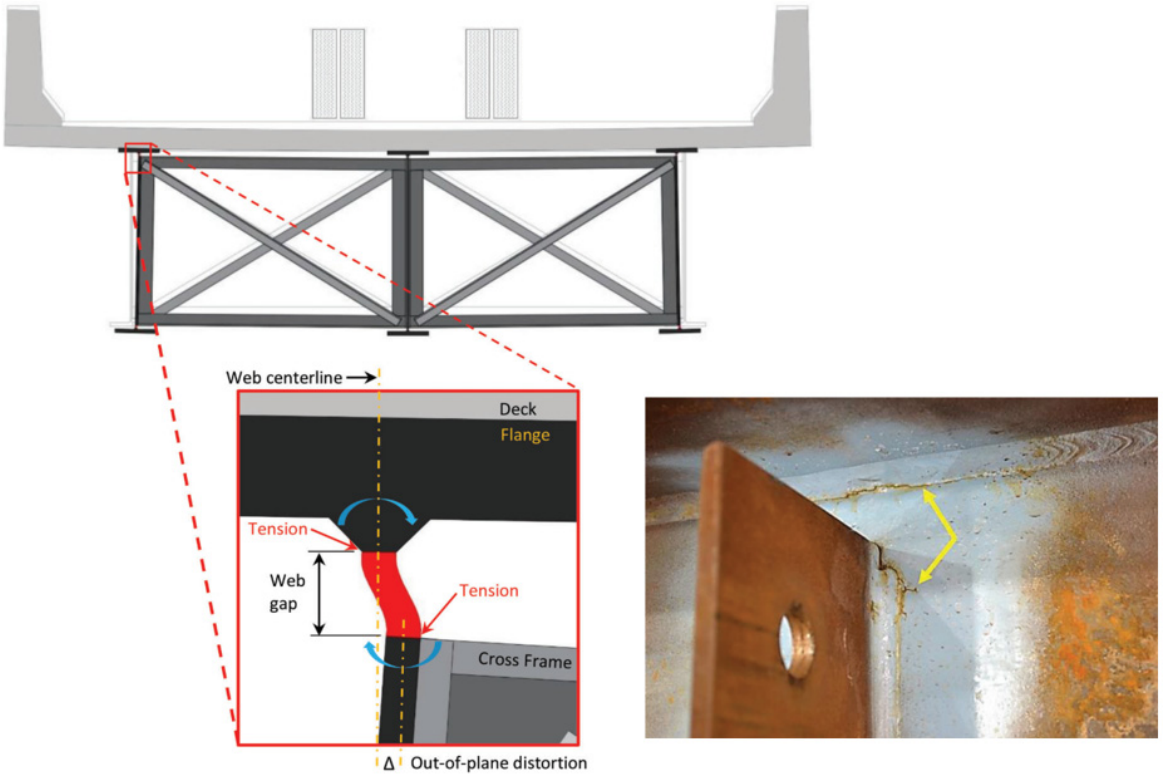


Figure 2. An example of fatigue-prone zone at the connection of the stiffener to the girder web [7].

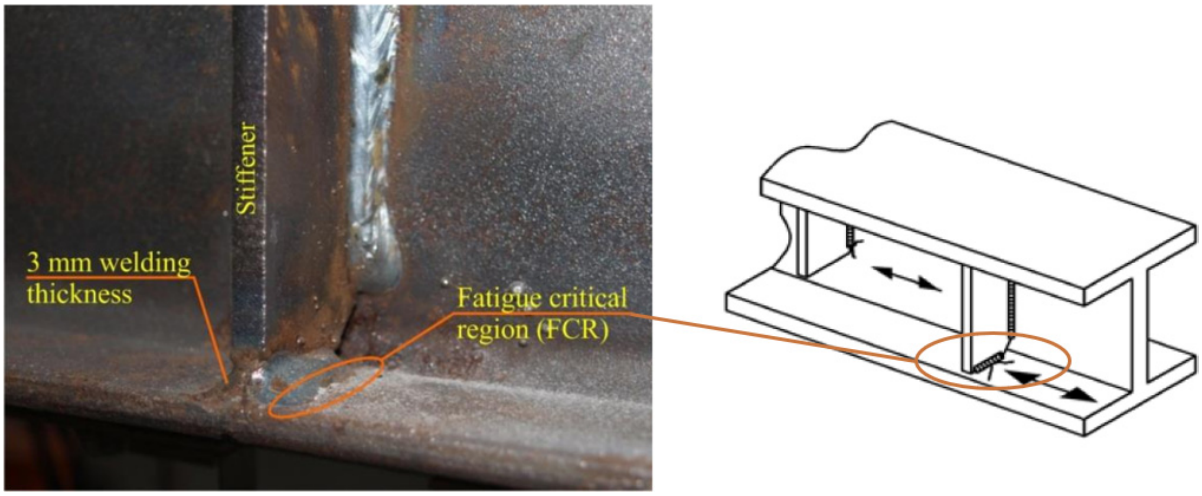


Figure 3. An example of fatigue-prone zone at the connection of the stiffener to the steel I-girder flange [2,8].

The differential deflections between adjacent girders at the cross-frame locations increase with the skew angle [9], leading to distortion-induced fatigue at the location of intermediate cross-frame connections. This type of fatigue, responsible for about 90% of fatigue cracking in steel bridges, results from out-of-plane forces transmitted through cross-frames, causing secondary stresses and cracking [10–12].

The severity of distortion-induced fatigue in skewed bridges can be affected by several factors. A major influencing factor is the geometry of the bridge, including parameters such as skew angle, span length between supports, spacing between adjacent girders, cross-frame layout, and thickness of the bridge deck. Larger skew angles result in increased differences in bending moments and deflections between adjacent girders under uniform

loading conditions, heightening susceptibility to distortion-induced fatigue. While the design for load-induced fatigue is focused on the stress range and expected number of cycles over the life of the bridge, distortion-induced fatigue is generally controlled by proper detailing to minimize the distortion. A recent study by McConnell and Almoosi (2022) [13] investigated distortion-induced fatigue in a skewed steel I-girder bridge using field testing and finite element modeling and it considered the details of connection plates, which are web stiffeners used to connect cross-frames to the girders. The results show that modern connection details with full-depth connection plates welded to both flanges generally mitigate distortion effects, except at highly skewed bent plate connections. Comparing inline and staggered cross-frames revealed increased principal stress ranges exceeding recommended thresholds at web locations with staggered frames in higher skew bridges. This indicates that staggered cross-frames may increase distortion-induced fatigue susceptibility despite other advantages with these layouts. The study provides important insights into detailing practices to control distortion in skewed steel bridges [13].

In steel bridges with skewed piers and abutments, cross-frames or diaphragms at the supports are typically oriented parallel to the skew angle. An important design consideration for fatigue exists in the connections between cross-frames and continuous steel girders at the interior supports. Specifically, the top flange of these girders above the interior supports experiences significant tensile stress range cycles due to live load effects, necessitating considerations to prevent crack growth due to fatigue. This scenario demands that the design of cross-frame connections to steel I-girders not only efficiently addresses forces and distortions but also safeguards the integrity of the girder flanges considering fatigue.

This paper investigates the behavior of the tension flange at interior piers of continuous skewed bridges. After a review of pertinent studies documented in the literature is provided in the next section, the results of finite element analyses considering nonlinear geometrical effects on 26 representative skewed bridges located in the State of Florida are utilized to quantify top-flange stress ranges based upon the passage of the fatigue design truck. The 26 bridges provide a robust sample that provides a good sample of geometrical variations found in practice, including skew angle, radius of curvature, girder spacing, and number of spans. For these analyses, comprehensive modeling of all bridge components is carried out, including the concrete deck, steel girders, cross-frames, bearings, and intermediate supports. In addition to the flange stress ranges, the range of axial forces in skewed end cross-frame members due to fatigue truck loading is compiled. Statistical analysis of the stress ranges and axial forces provides distributions and maximum expected values useful for fatigue research and development. The paper ultimately presents observations and conclusions regarding the fatigue performance of the tension flange detail in skewed continuous span girders. Specific recommendations are made regarding allowable stress range thresholds and detailing practices to mitigate distortion-induced fatigue. Directions for future research are also discussed, including experimental fatigue testing to further qualify the expected performance of novel connection details such as Half-Round Bearing Stiffeners (HRBS).

1.1. Background

1.1.1. Cross-Frames in Skewed Steel Girder Bridges

Cross-frames are important structural elements in steel girder bridges that provide lateral stability to the bridge girders and help distribute live loads and resist transverse loading [14]. In some instances, the cross-frames can potentially provide for reserve stiffness and capacity after certain failure mechanisms [15]. There are a variety of geometrical configurations that are used for cross-frames. A very common geometry consists of a top chord, a bottom chord, and a pair of diagonal members, arranged in an X-type truss configuration as depicted in Figure 4 [16]. Alternatively, cross-frames may also adopt a K-frame geometry as shown in Figure 5. The truss members in cross-frames are most often single-angle members, but also may consist of channel, double angles, W-shapes, or WT-Shapes [16].

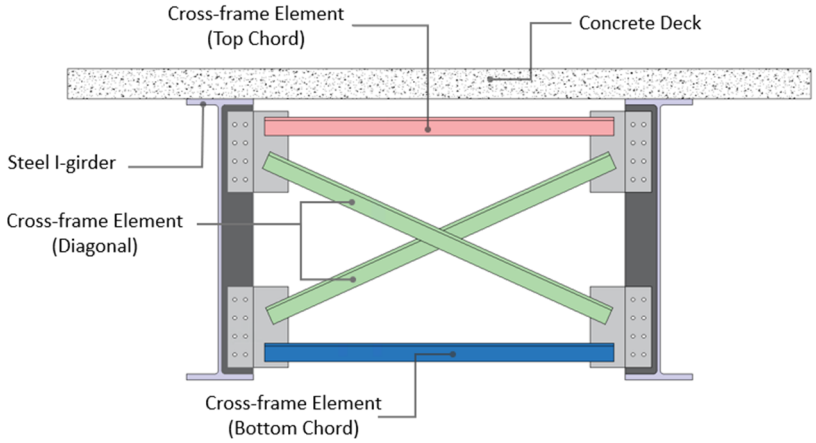


Figure 4. X-type cross-frame configuration (No scale).

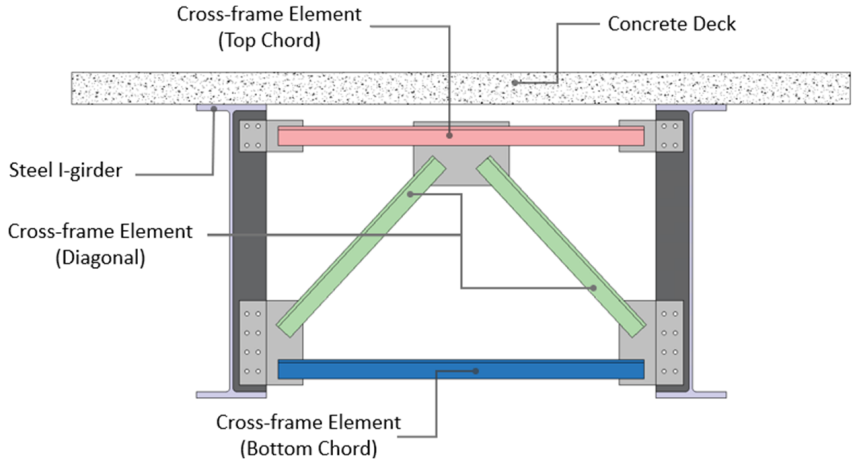


Figure 5. K-frame Cross-Frame Configuration (No scale).

In addition to cross-frames, diaphragms are also a common bracing system in steel bridges (Figure 6). While cross-frames derive their stiffness from truss action, diaphragms provide bracing through flexural or shear stiffness. Shallow diaphragms resist distortion through flexural resistance, whereas deeper diaphragms rely on shear stiffness in the web of the diaphragm.

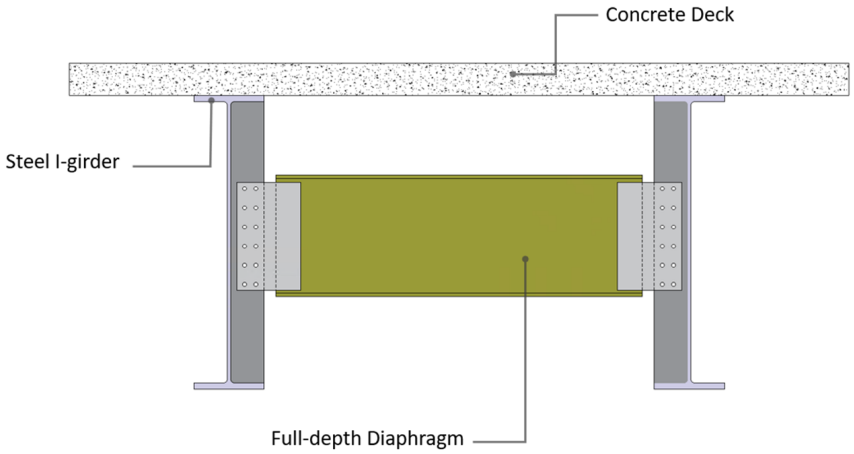


Figure 6. Full-depth diaphragm member detailing (No scale).

End cross-frames are typically defined as truss members located at the end of each bridge span. In a multi-span bridge, end cross-frames would be located at the end supports (abutments) and intermediate supports (piers). On the other hand, other cross-frames located in between the bridge supports along the bridge spans are defined as intermediate cross-frames. As noted earlier, if the bridge skew angle is more than 20°, intermediate cross-frames must be placed perpendicular to the steel girders (AASHTO LRFD 6.7.4.2 [2]), while end cross-frames should be in line with the support centerline (Figure 7).



Figure 7. End cross-frame location in a steel bridge with 60° skew in Lubbock, TX [17].

The focus of this study is specifically directed toward bridges equipped with X-frame and K-frame end diaphragms. Bridges with full-depth diaphragms at the supports are not considered. The major roles of end diaphragms include controlling the twist of the girders, supporting the deck and expansion joint, and transferring lateral loads such as seismic and wind loads from the bridge deck to the bearings. Astaneh-Asl [18], Bruneau [19], and Shinozuka [20] have shown seismic load transferring and the importance of the end cross-frame design [21] by reporting damages within end cross-frames during severe earthquakes.

1.1.2. Skewed Connections in Bridges

In a standard steel connection such as cross-beam to girder, beam to girder, or beam to column, the structural elements are generally connected at an angle of 90 degrees. However, some structures and bridges in certain circumstances have elements that do not have a perpendicular connection to other elements. A connection that links two elements at an angle other than a right angle is called a skewed connection. In order to ensure safety and economical construction, the application of skewed connections often requires unique design considerations [22].

In bridges with skewed supports, geometric requirements often call for skewed connections between the end cross-frames and girders. As noted earlier, when the skew angle is larger than 20 degrees, the AASHTO LRFD Bridge Design Specifications [2] require intermediate cross-frames to be oriented perpendicular to the girder, but the end cross-frame or diaphragms usually frame in at an angle equal to the skew angle. In addition to the conventional and newly recommended details for steel girder bridges with skewed supports discussed in the following sub-sections, there are also some innovative connections that have recently been suggested [23,24]. However, these require further investigation prior to implementation. These connections vary in terms of their performance and ease of installation.

Bent Plate Connection

As noted above, for skew angles larger than 20 degrees, AASHTO LRFD [2] requires intermediate cross-frames to be aligned perpendicular to the girders. End cross-frames, regardless of skew angle, must be parallel to the skew and hence in line with the supports or abutment center line. This implies that the end cross-frames will connect the girder at a non-perpendicular angle, potentially causing welding and fit-up complications. Bent plates (as shown in Figures 8 and 9) between the cross-frame braces and stiffeners are commonly used to facilitate the connection, resulting in perpendicular orientations of the stiffeners [25]. Although bent plates make the fabrication easier, they can reduce the cross-frame effectiveness due to their flexibility.

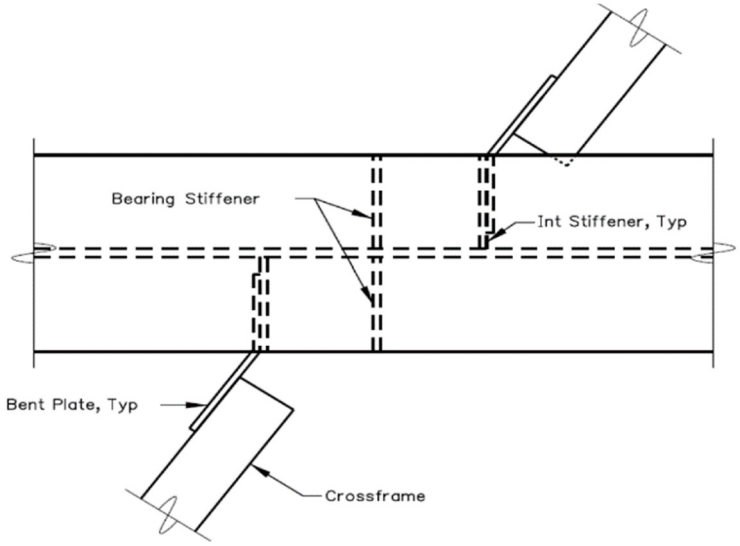


Figure 8. Skewed end cross-frame bent plate connection [17].



Figure 9. Bent plate end cross-frame connection.

Although a bent plate will often suffice for small skew angles, significant issues can arise for highly skewed bridges [17]. Experimental studies and finite element modeling (FEM) results have shown that the main cause of out-of-plane bending and deformation of the elements is the eccentricity of the bent plate connection [26]. Eccentric connections cause member bending, which has a negative impact on stiffness, fatigue performance, and strength.

Half-Round Bearing Stiffener Connections (HRBS)

In an extensive research study, Quadrato et al. (2010) [17,27] investigated existing connection details for end cross-frames to steel girders in heavily skewed systems and considered new details. The study focused on bent plate connections and proposed a new Half-Round Bearing Stiffener (HRBS) detail to facilitate connection fabrication in skewed girder applications. The configuration of this connection assures the connection stiffener plate is perpendicular to the half-round plates regardless of the skew angle and avoids the use of bent connection plate (Figure 10).



Figure 10. Small-scale connection test specimens by Quadrato et al. [17].

In addition to improved constructability, there are also structural advantages to utilizing curved stiffeners. The large-scale test demonstrated the effect of the HRBS in increasing the warping restraint for the girder, therefore improving the lateral-torsional buckling resistance of the girders (Figure 11). The HRBS also showed lower values of the end twist for the girders compared to girders with conventional plate stiffeners and bent plate connections. Also, staggering the intermediate cross-frames was shown to have reduced the intermediate cross-frame forces but it did not significantly impact the girder end twist.

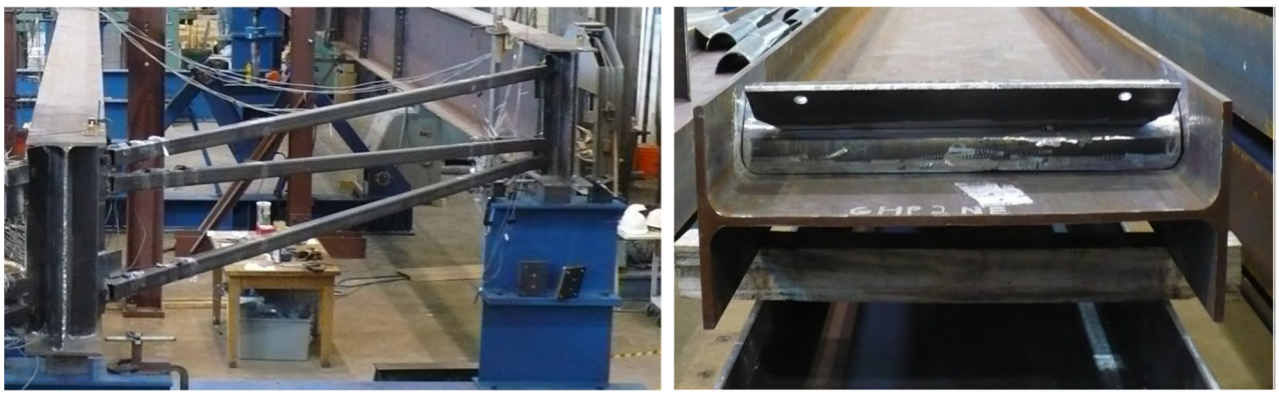


Figure 11. Large-scale test specimen with the HRBS (**left**) and a single stiffener prepared for welding (**right**) Quadrato et al. [17].

Quadrato et al. used finite element (FE) models to validate experimental results on cross-frame and girder connections, focusing on elastic, eigenvalue buckling, and nonlinear geometric analyses (Figure 12). Their study, which included comparisons of the HRBS and bent plate connections, led to the development of design guidelines for end cross-frame connections. The study included parametric analyses on various girder cross-sections and skew angles, assessing the effect of factors such as plate thickness and bend radius on stiffness. The HRBS connection was found to offer higher connection stiffness and improved warping stiffness in girders, enhancing the buckling strength and reducing girder twist and cross-frame forces. Additionally, the research evaluated fatigue performance in the HRBS connections, especially at interior girder supports. Comparing stress concentrations in the HRBS versus inclined plate stiffeners, the researchers concluded that the HRBS detail fits into the AASHTO's Fatigue Category C, suggesting its suitability over bent plates in terms of fatigue resistance [17].

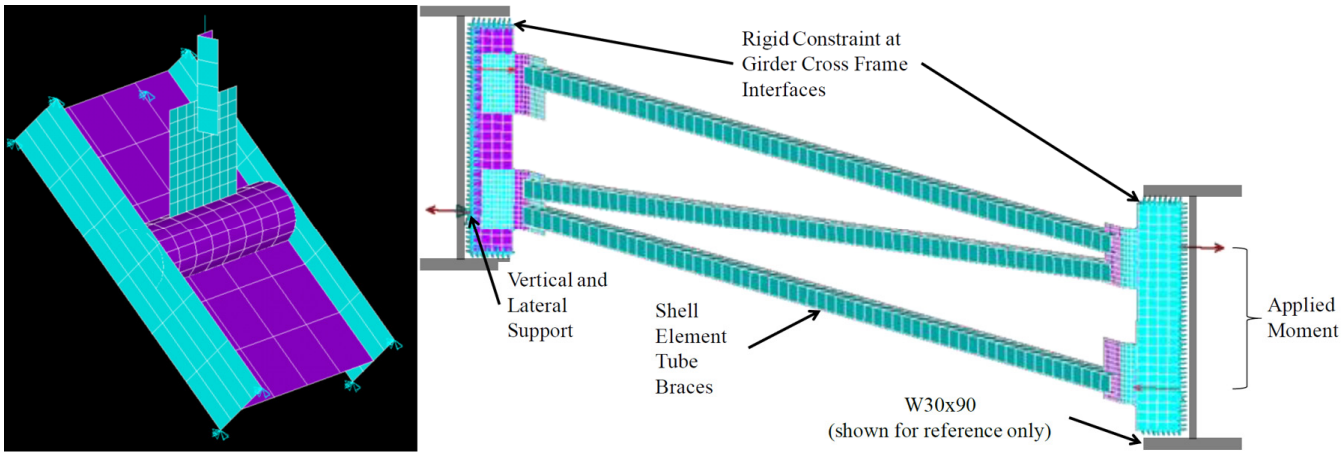


Figure 12. Finite element models of the HRBS connection (**left**) and an end cross-frame to girders (**right**) Quadrato et al. [17].

2. Methodology

2.1. Selection of the Representative Bridges for Analytical Study

Before a discussion of the analytical investigation is provided, the representative bridges to be analyzed that cover the practical range of the major parameters of continuous skewed steel girder bridges need to be identified. These parameters include skew angle, type of continuous spans (one-sided or two-sided continuity), span length, bridge width, number of steel girders, cross-frame configuration, and girder spacing. The Florida Department of Transportation (FDOT) research identified 26 bridges to be considered, providing a good representation of the range of geometries found in practice. The list of bridges adopted for this study with the alternative numbering to be referred to hereafter is shown in Tables 1 and 2. The analysis of these bridges is focused on evaluating the behavior of the half-round stiffener connection for potential use with bridges with similar geometries. The table also includes information on the number of spans, span lengths, skew angle and index at piers and abutments, curvature (angle, radius, and span/radius ratio), total width, framing width, number of girders, and number of lanes.

Table 1. Bridge matrix and geometry information used for the analytical study (Part 1).

Bridge Number	Span Length (ft)					Skew Angle at Pier (Degree)					Curvature		
	Span 1	Span 2	Span 3	Span 4	SUM	Bent/ Pier 1	Bent/ Pier 2	Bent/ Pier 3	Bent/ Pier 4	Bent/ Pier 5	θ	R (ft)	L/R
1	190	140	-	-	330	52.8	56.1	57.2	-	-	1°44′46″	3281.4	0.058
2	204	160	-	-	364	56.2	56.2	56.2	-	-	-	-	0
3	123	137	-	-	260	23.0	23.0	23.0	-	-	-	-	0
4	217	234	-	-	450	39.8	39.8	39.8	-	-	-	-	0
5	210	234	-	-	445	36.1	39.2	42.7	-	-	1°30′0″	3819.7	0.061
6	186	167	156	-	509	40.8	27.0	0.0	0.0	-	4°45′0″	738.2	0.252
7	218	250	-	-	468	40.6	45.0	45.0	-	-	1°59′59″	2865.0	0.087
8	187	154	149	-	491	41.1	50.9	34.7	0.0	-	5°	1145.9	0.163
9	159	239	235	176	809	0.0	57.0	50.5	39.7	0.0	8°14′38″	695.0	0.344
10	198	213	-	-	411	44.1	48.7	46.8	-	-	7°04′25″	810.0	0.263
11	172	253	253	202	880	0.0	50.1	50.1	50.1	0.0	-	-	0
12	189	157	159	228	732	53.0	36.0	8.0	45.0	45.0	15°34′32″	5725.1	0.040
13	156	145	-	-	301	40.5	40.5	40.5	-	-	-	-	0
14	172	172	-	-	343	55.0	55.0	55.0	-	-	-	-	0
15	262	255	-	-	517	52.2	53.3	54.7	-	-	0°29′14″	11,758.0	0.022
16	178	178	-	-	355	25.6	25.6	25.6	-	-	-	-	0
17	253	253	-	-	505	50.4	50.4	50.4	-	-	-	-	0
18	252	252	-	-	503	50.2	50.2	50.2	-	-	-	-	0
19	149	174	-	-	323	23.4	23.4	23.4	-	-	-	-	0
20	230	210	-	-	440	43.8	43.8	43.8	-	-	-	-	0
21	208	209	-	-	416	36.7	36.0	35.3	-	-	-	-	0
22	170	170	-	-	340	52.7	52.7	52.7	-	-	-	-	0
23	199	199	-	-	398	54.5	54.5	54.5	-	-	-	-	0
24	181	174	-	-	355	25.0	0.0	25.0	-	-	1°48′	3183.1	0.057
25	167	185	-	-	353	35.5	35.5	35.6	-	-	-	-	0
26	204	196	185	-	585	44.2	44.7	58.7	58.7	-	-	-	0

Table 2. Bridge matrix and geometry information used for the analytical study (Part 2).

Bridge Number	Girder Spacing (in.)	No. of Lanes	No. of Girders	Deck Width (ft)	w_g (ft)	Skew Index (Is) $Is = w_g \cdot \tan q/Ls$				Max Skew Index (Is)	End Cross-Frame Type
						Span 1	Span 2	Span 3	Span 4		
1	123	3	6	58.2	51.3	0.40	0.57	-	-	0.57	Inverted-V
2	114	3	6	54.3	47.5	0.35	0.44	-	-	0.44	Inverted-V
3	120	2	4	37.1	30.0	0.10	0.09	-	-	0.10	V
4	144	3	5	56.1	48.0	0.18	0.17	-	-	0.18	V
5	144	4	6	67.1	60.0	0.23	0.24	-	-	0.24	V
6	150	2	4	48.4	37.4	0.17	0.11	-	-	0.17	V
7	132	1	3	30.1	22.0	0.10	0.09	-	-	0.10	Inverted-V
8	111	2	5	43.1	37.0	0.24	0.29	0.17	-	0.29	V
9	144	1	4	44.0	36.0	0.35	0.23	0.19	0.17	0.35	Inverted-V
10	116	1	4	37.3	29.0	0.17	0.15	-	-	0.17	Inverted-V
11	144	2	4	43.1	36.0	0.25	0.17	0.17	0.21	0.25	V
12	148	3	5	60.2	49.2	0.35	0.23	0.31	0.22	0.35	Inverted-V
13	117	2	5	47.1	39.0	0.21	0.23	-	-	0.23	V
14	150	2	4	47.1	37.5	0.31	0.31	-	-	0.31	Inverted-V
15	144	2	4	43.1	36.0	0.18	0.20	-	-	0.20	Inverted-V
16	161	2	4	50.2	40.3	0.11	0.11	-	-	0.11	Inverted-V
17	140	2	6	65.0	58.3	0.28	0.28	-	-	0.28	Inverted-V
18	153	2	5	59.0	51.0	0.24	0.24	-	-	0.24	Inverted-V
19	160	4	8	101.1	93.3	0.27	0.23	-	-	0.27	Inverted-V
20	127	4	7	71.1	63.4	0.26	0.29	-	-	0.29	Inverted-V
21	127	3	6	59.1	52.9	0.19	0.18	-	-	0.19	Inverted-V
22	97	2	7	55.3	48.3	0.37	0.37	-	-	0.37	Inverted-V
23	141	2	4	43.1	35.3	0.25	0.25	-	-	0.25	Inverted-V
24	96	1	4	30.1	24.0	0.06	0.06	-	-	0.06	Inverted-V
25	108	3	6	54.4	45.1	0.19	0.17	-	-	0.19	Inverted-V
26	105	2	5	42.5	35.0	0.17	0.29	0.31	-	0.31	Inverted-V

2.2. FEM Modeling

For finite element (FE) analysis, the research team gained access to a few viable finite element analysis programs for consideration of their use in the analyses. Two of the programs that were considered were mBrace3D [28] and MIDAS Civil [29]. One of the representative bridges was selected as a benchmarking case to evaluate these FE programs. The preliminary analyses that were performed on this bridge showed agreement between

different programs. For this study, because of the easier input along with better modeling options, the MIDAS program was selected to carry on with the main body of the analysis.

There have been earlier attempts to analyze the effect of cross-frames in general and skewed end cross-frames in particular. One of these studies (NCHRP 725- FDOT Report) used various methods, including the grid model and 3D finite element method, in which only the girder web was modeled with plate elements, and the beam element was used for other components. The analysis results obtained in the study reported in this paper using more sophisticated modeling, i.e., plate element for deck, girder web, and girder flange, were compared to the results of the previous work, and a good agreement was observed. Additionally, for the selected FE program, various modeling approaches were applied in a preliminary analysis including the type of FE elements and modeling of the support conditions. The results were compared, and the most effective method was selected to continue with the analysis of all 26 bridges.

There are several options for FE modeling of bridges. These include type of FE elements for the girder, deck, and bracing, as well as support conditions. To select the most appropriate and representative option, a skew steel girder bridge was selected for preliminary analysis using advanced 3D finite element analysis (FEA) with MIDAS Civil Software [29]. Selective modeling options were adopted and compared to investigate the sensitivity of the model to various conditions related to the stress ranges in the top flange of the girder over the intermediate pier. Figure 13 shows the 3D FEM model of this bridge. The global coordinate system of the FE model is shown in the figure. Three types of support conditions were compared: Case A—simple rigid supports, Case B—neoprene bearings over rigid supports, and Case C—neoprene bearings over the pier, as shown in Table 3. For Case C, the pier substructure was also modeled. Moreover, for considering the type of FE element, two cases were modeled, one with plate elements for all members except the cross-frame members that were modeled as beam elements. For the other case, deck and girder webs were modeled using plate elements, and a beam element was used for modeling girder flanges and cross-frame members. Table 4 contains the factored fatigue stress ranges for combinations of support and element type conditions. The results show that firstly, simplifying the modeling of girder flanges using beam elements alters the results noticeably. Therefore, it was decided to model the bridges using plate elements for all members except for the cross-frames. Secondly, simplifying the support condition with the use of rigid supports changes the results considerably and should not be adopted. On the other hand, there is negligible difference in the results between the models with and without pier substructure. Hence, the model using neoprene bearings over rigid supports was used for subsequent analyses.

Table 3. Substructure and supports for FEM modeling assumption case properties.

Case Name	Rigid Supports	Neoprene Bearings	Piers Modeled
Case A	✓ *	-	-
Case B	-	✓	-
Case C	-	✓	✓

* Symbol "✓" indicates that the condition is applicable to the case.

Table 4. Factored fatigue stress range at the top flange on the intermediate piers (ksi).

Case	1 Plate: Deck, Girder Web, and Flanges Beam: Cross-Frames	2 Plate: Deck and Girder Web Beam: Girder Flange & Cross-Frames
A Simple Rigid Support	1.45	1.22
B Neoprene Bearing	1.39	1.44
C Piers Modeled	1.40	1.57

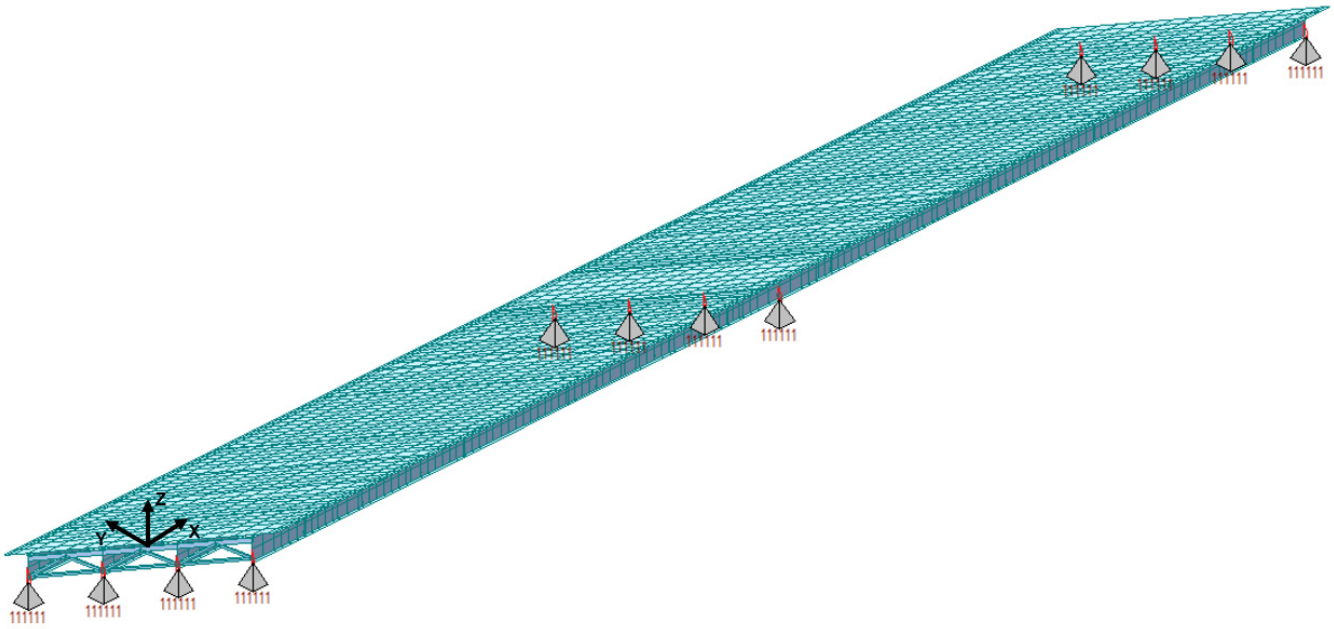


Figure 13. 3D FEM steel I-girder bridge model.

After identifying the appropriate modeling options through preliminary analysis, the comprehensive modeling of all 26 bridges was performed. The structural configuration of the selected skew bridges comprises continuous steel I-girders interconnected by intermediate cross-frames and end cross-frames, topped with a concrete deck. The support condition was modeled using neoprene bearing pads over rigid supports.

2.2.1. General Assumptions

Structural Elements

All bridges were modeled using plate elements to accurately represent the concrete decks, top and bottom flanges, and the web of the steel I-girder, with a mesh size of approximately 50 inches, as shown in Figure 14. Additionally, beam elements were employed for the cross-frame members, encompassing the top and bottom chords along with diagonal members. The study also incorporated the specific cross-frame configuration as depicted in the design drawings, which included various types of braces such as X-frames, K-frames, or inverted K-frames. To assess the structural response and stability of these bridges, a thorough linear static analysis was methodically conducted.

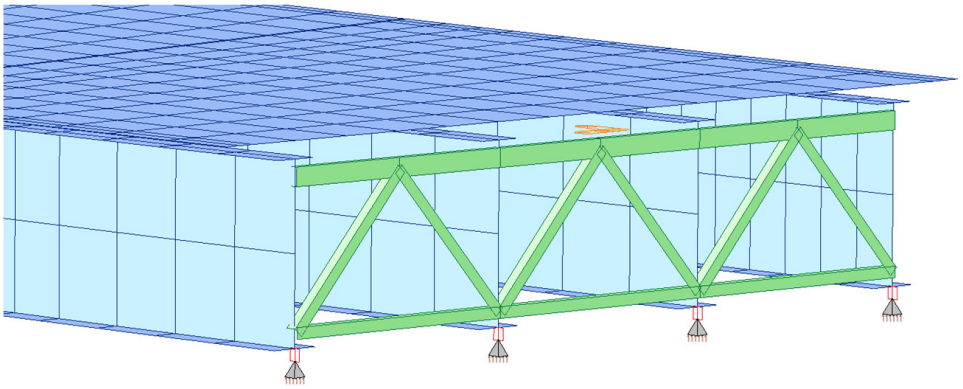


Figure 14. 3D FEM steel I-girder bridge model using plate and beam elements.

In the development of the 3D models, careful consideration was given to the effects of connection eccentricity on the axial rigidity of the cross-frame members, as illuminated

by the works of Wang et al. (2012) and the National Cooperative Highway Research Program Report No. 962 (NCHRP, 2021) [30]. These studies underscored the impact of end connection eccentricities on the axial rigidity of single-angle and flange-connected tee-section cross-frame members, leading to a reevaluation of stiffness parameters in the bridge analysis. Consequently, modifications to the axial rigidity were incorporated into the models, adhering closely to the guidelines set forth in AASHTO LRFD [2] Article 4.6.3.3.4c and the associated commentary, and NCHRP 962 [30]. In this context, the focus was primarily on the composite condition of the structures in service. An axial stiffness modification factor of 0.75, as recommended for composite conditions, was uniformly applied to all relevant cross-frame members. This approach was selected based on the conservative nature of the modification factor for composite conditions, aligning with the specific requirements and characteristics of the bridges under consideration.

Materials

Two primary structural materials, steel and concrete, were used to model these bridges. Both materials were assumed to be linear elastic based upon the combined effects of construction and service load levels from the passage of the AASHTO fatigue truck. The properties of the materials are shown in Table 5. These properties were consistent with 24 of the 26 bridges based on information in the design drawings. The specified material strengths on the other 4 bridges only differ marginally.

Table 5. Material properties.

Material	Strength (ksi)	Modulus of Elasticity (kips/in^2)	Poisson's Ratio	Weight Density (kips/ft^3)	Damping Ratio
Steel	$F_y = 50$	2.90×10^4	0.3	0.49	0.02
Concrete	$f'_c = 4.5$	3.86×10^3	0.2	0.15	0.05

Dimensions and Quantities

For all bridges, the dimensions for span length, support skew angle, radius for curved bridges, deck width, girder spacing, number of girders, deck thickness, and haunch heights were taken into account in accordance with the information provided in the design drawings. The top 0.5 in. of the bridge deck slab thickness was considered sacrificial and included in the dead load of the deck slab but was not considered in the computation of the section properties of the slab or the composite section properties of the girders.

The selected bridges were modeled with intermediate cross-frames, skewed cross-frames over piers, and abutments as specified in the bridge plans. It is important to note that in three of the bridges, design drawings did not indicate any skewed cross-frames over the piers. For these systems, skewed cross-frames were still modeled, assuming member sizes similar to those in the cross-frames over the abutments in the bridge. The geometry of the intermediate cross-frames modeled in each span was close to values obtained from the design drawings. Although in some cases the plans had variations in the intermediate cross-frame spacing, equally spaced cross-frames were modeled based upon the FEM program modeling interface, resulting in slight differences from the spacings shown on the drawings.

2.2.2. Fatigue Loading

Variation in tensile stresses under live loading is the main precursor for the fatigue of the top flange of a girder at the negative moment region over an intermediate pier, as well as the design of the cross-frame connection at this location. While for the AASHTO LRFD Strength 1 design [2], loading consisting of multiple trucks on either side of the negative moment region and in multiple lanes is required, the AASHTO LRFD [2] methods for fatigue design consider the passage of a single fatigue truck. In other words, the fatigue

truck is modeled considering passage along each potential lane individually to develop an envelope that represents the critical position of the truck for fatigue in a given cross-frame. The AASHTO BDS identifies the fatigue truck as a HS20 truck (Figure 15) for which the spacing between the second and third axles is 30 ft. Longitudinal positioning of the truck is selected based upon the critical stress range for the detail of interest. This position is not based upon striped lanes but at a constant transverse position that creates the critical results.

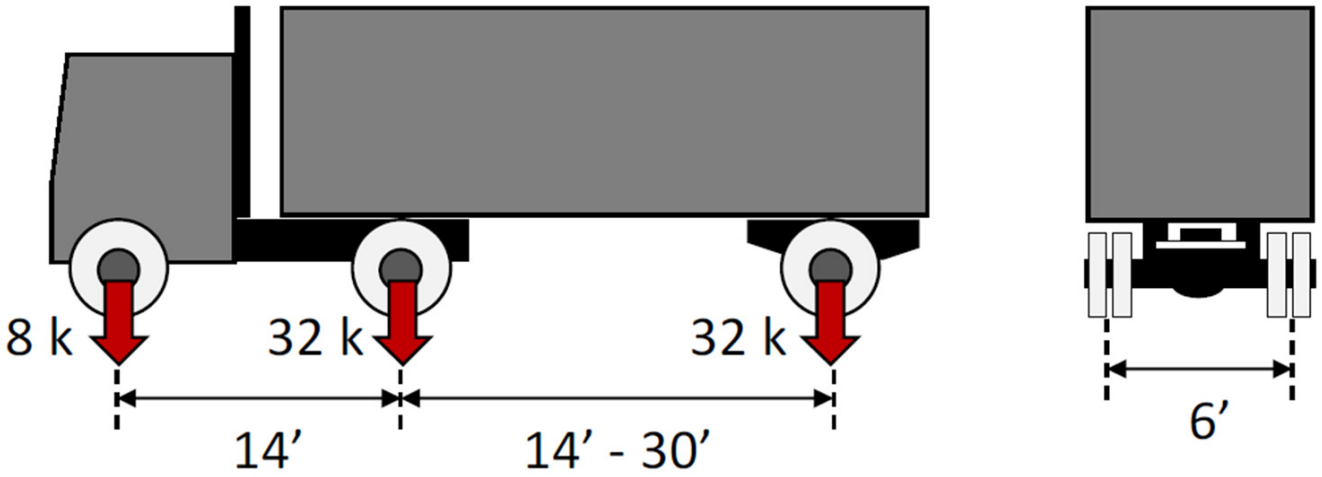


Figure 15. HS–20 Design truck load.

According to Section 3.4.1 of the AASHTO LRFD [2] Bridge Design Specifications, it is required that the stresses obtained from fatigue truck loading be multiplied by a factor of 1.75 for Fatigue–I design, which pertains to the combination of fatigue and fracture loads related to infinite load-induced fatigue life, and a factor of 0.8 for Fatigue II, which relates to the combination of fatigue and fracture loads related to finite load-induced fatigue life. Furthermore, for fatigue design, it is necessary to take into account the Dynamic Load Allowance (IM) multiplier equal to 1.15.

3. Results and Discussions

3.1. Fatigue Stress Ranges in Top Flanges over Skewed Piers

The determination of the fatigue stress range in top flanges over skewed supports involved calculating the maximum and minimum stress in that element when a fatigue truck traversed the bridge in a specific lane. Separate calculations of the stress range for each lane were conducted to determine the critical location. The study employed an influence surface analysis to ascertain the maximum and minimum impact of the fatigue truck on top flanges over skewed supports. A representative influence surface is shown in Figure 16. The figure shows the influence surface for the top-flange plate element internal stress over the exterior left support in Bridge 23. Figures 17 and 18 depict the location of the fatigue truck in the first lane, corresponding to the maximum and minimum stress in that element. This procedure was replicated for other transverse lanes to identify the most critical stress range for the element.

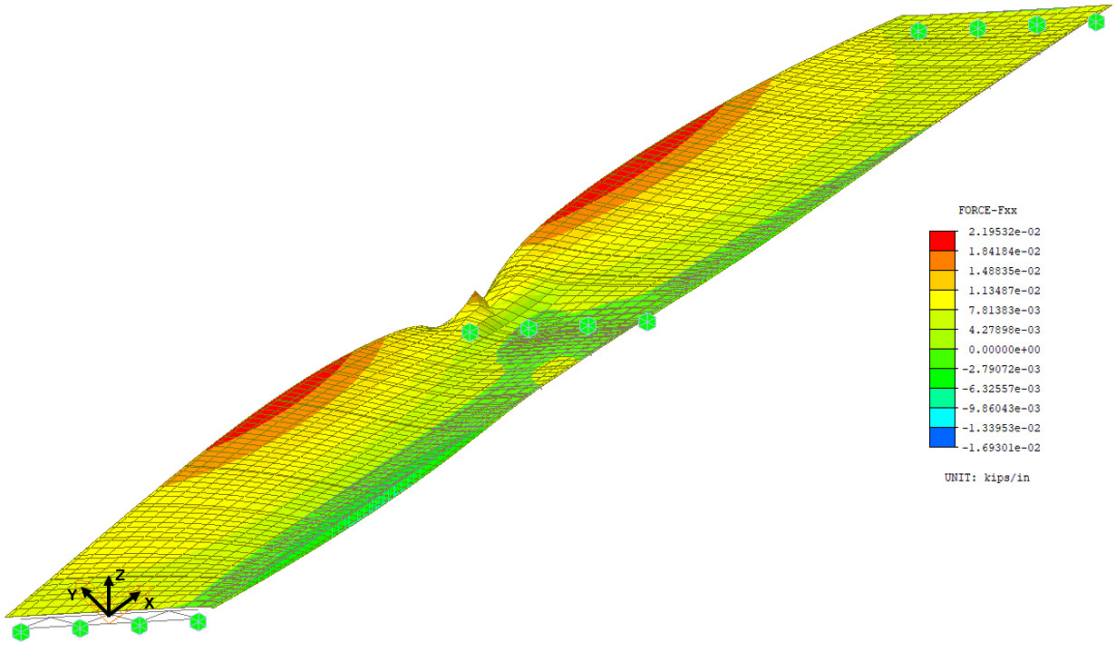


Figure 16. Influence surface for the longitudinal force in the top flange element over the skewed support in the first lane of Bridge No. 23.

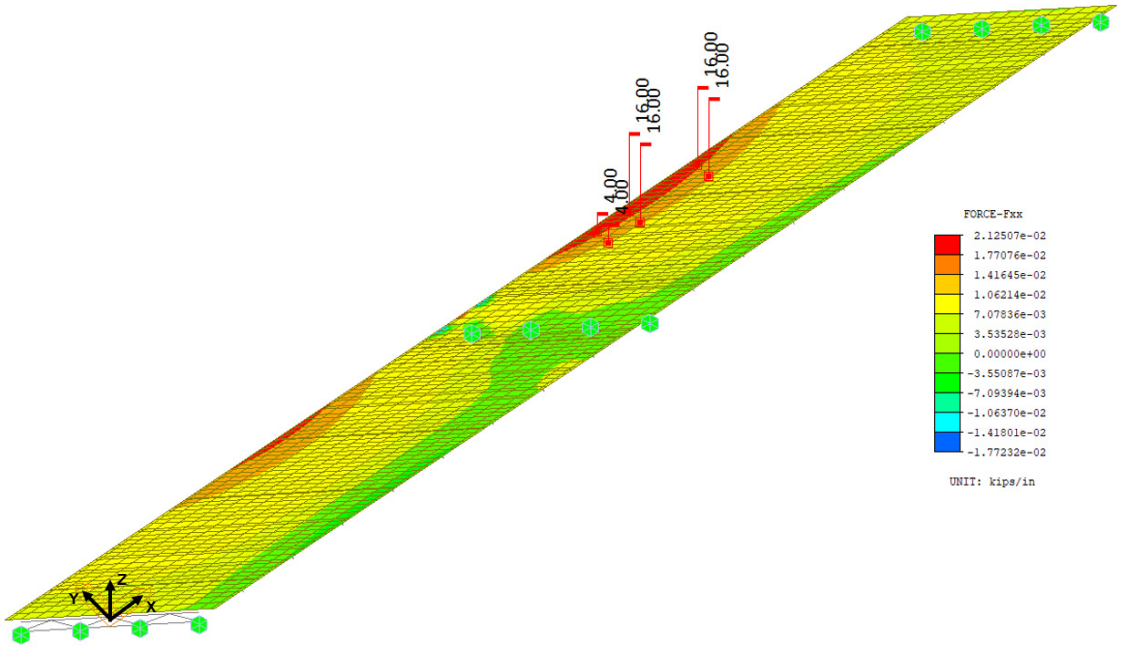


Figure 17. The optimal position of the fatigue truck in the first lane of Bridge No. 23 to maximize stress in the top flange of the steel I–girder over the skewed support.

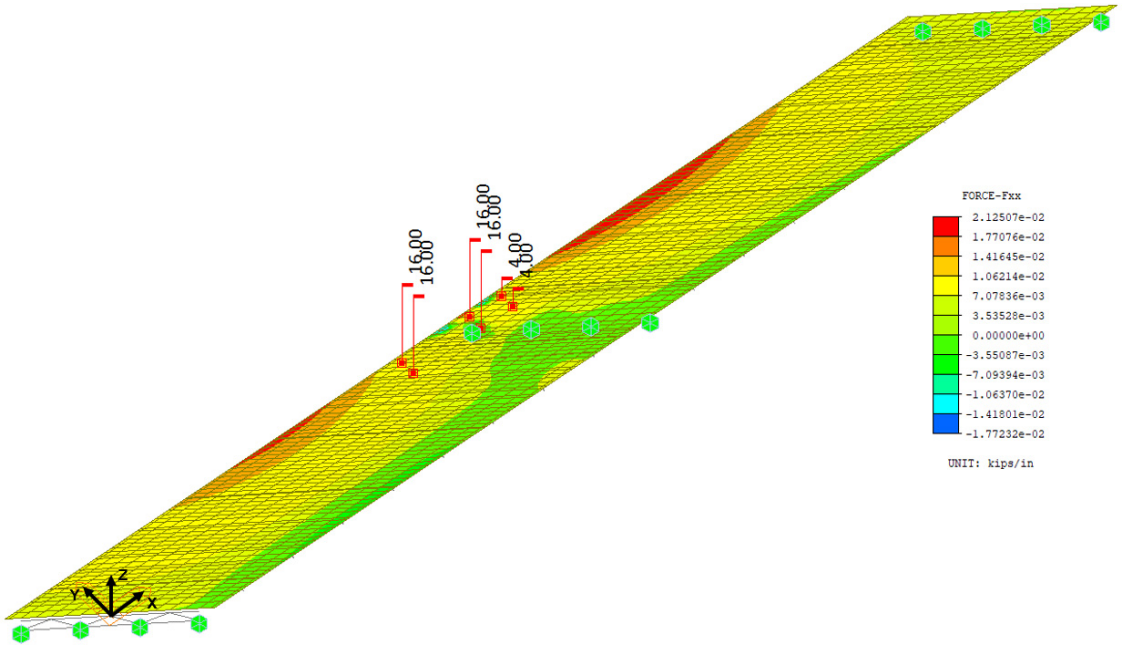


Figure 18. The optimal position of the fatigue truck in the first lane of Bridge No. 23 to minimize stress in the top flange of the steel I–girder over the skewed support.

As previously discussed, a primary focus of the fatigue assessment is the top flange located over the piers, particularly due to the tensile stresses arising from negative moments in that region. To thoroughly understand the fatigue performance of top flanges, the stress ranges were calculated based on the local stresses in the elements immediately above the supports, accounting for the element's local axis orientation. The stress range in the plane of the top flange was calculated by finding the difference between the highest and lowest local stress values in each main local direction. This was achieved using Equations (1)–(3), where Δf_x, and Δf_y represent the stress ranges in the x and y directions, respectively, and Δf_{xy} represent the shear stress range. $\sigma_{x\text{-}max}$ and $\sigma_{y\text{-}max}$ denote the maximum local stresses in the x and y directions, while $\sigma_{x\text{-}min}$ and $\sigma_{y\text{-}min}$ indicate the minimum local stresses in these directions. Once the stress ranges for both directions are obtained, their resultant is computed and considered as the overall stress range (Δf) in the element based on Equation (4). It should be noted that tensile stresses were considered positive and compressive stresses negative. Hence, the results are based on the absolute stress range, i.e., if the minimum stress was compressive, its value was added to the tensile stress.

$$\Delta f_x = \sigma_{x-max} - \sigma_{x-min} \tag{1}$$

$$\Delta f_y = \sigma_{y-max} - \sigma_{y-min} \tag{2}$$

$$\Delta f_{xy} = \sigma_{xy-max} - \sigma_{xy-min} \tag{3}$$

$$\Delta f = \frac{1}{2}\left(\Delta f_x + \Delta f_y\right) + \frac{1}{2}\sqrt{\left(\Delta f_x - \Delta f_y\right)^2 + 4\left(\Delta f_{xy}\right)^2} \tag{4}$$

Upon computing the Fatigue–I stress ranges for the top flanges across all 26 representative skewed bridges, the largest value for each bridge was identified. This maximum stress range represents the most significant stress range that occurs in the top flange directly over the intermediate supports. A conservative approach was utilized considering the envelope of minimum and maximum stresses for the stress range calculation. Table 6 compiles these peak values, and Figure 19 (the histogram) depicts the distribution of these maximum factored stress ranges. The horizontal axis (x-axis) of the histogram represents the range of top-flange fatigue stress in ksi divided into six intervals, while the vertical axis (y-axis)

indicates the number of bridges that fall within each stress range interval. The range of values is between 1.24 and 3.63 ksi, with an average value of 2.41 ksi.

Table 6. The top-flange maximum stress range over the intermediate supports for the Fatigue–I envelope.

Bridge Number	Maximum Top-Flange Fatigue Stress Range (ksi)	Bridge Number	Maximum Top-Flange Fatigue Stress Range (ksi)
1	2.23	14	2.53
2	1.24	15	2.42
3	1.60	16	1.84
4	1.70	17	2.04
5	1.93	18	1.46
6	2.86	19	2.17
7	3.63	20	2.76
8	3.17	21	2.48
9	2.84	22	1.66
10	3.14	23	3.13
11	1.94	24	3.57
12	2.40	25	2.90
13	2.35	26	2.79

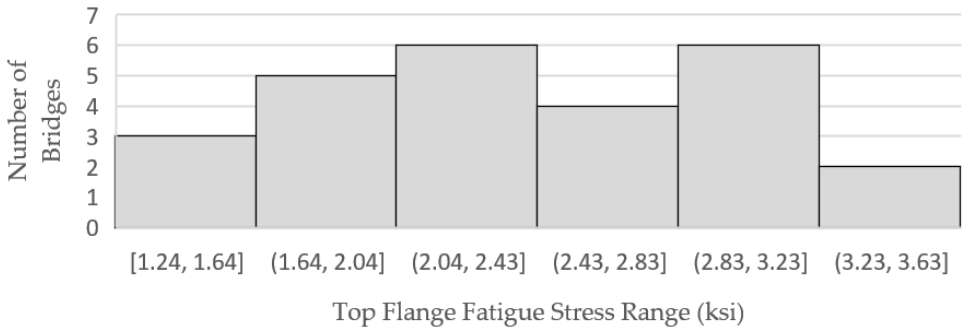


Figure 19. Maximum top-flange Fatigue–I envelope stress range (ksi).

The top flange in steel I-girder bridges with a stiffener plate perpendicular to the web is classified as Category C′, as per the criteria outlined in AASHTO LRFD Table 6.6.1.2.3-1 (4.1) [2], with a constant amplitude fatigue threshold (CAFT) set at 12 ksi. The CAFT is defined as the stress level below which a material can theoretically withstand an infinite number of load cycles without succumbing to fatigue failure. AASHTO Fatigue Category C (CAFT = 10 ksi) was also recommended by a recent study by Quadrado et al. [17] for steel girders with Half-Round Bearing Stiffeners (HRBS).

The analysis results show that the maximum fatigue stress range for top flanges positioned over skewed piers was 3.57 ksi, a value notably lower than the CAFT associated with such configuration. This finding suggests that fatigue in top flanges located over skewed intermediate bridge supports is not likely to be a problem. This in major part can be attributed to the presence of a solid slab atop the steel I-girder and a supporting element beneath the bottom flange in the specified area. These robust structures restrict movement or deformation of the steel I-girder, thereby mitigating the accumulation of stresses caused by differential deformation of girders, which is identified as a primary source of twisting in skewed bridges [31].

The above approach follows the screening method for fatigue-sensitive connections using normal stress based on S-N curves at a global scale. If a specific connection detail is in focus, a multi-scale modeling technique that bridges the gap between global structural behavior and local detail-specific responses can be beneficial. By incorporating both global

bridge models and finely meshed local models of critical details, multi-scale modeling provides a comprehensive view of the bridge behavior [32–37].

3.2. Cross-Frame Forces for Fatigue Envelope

Determining the precise internal forces acting on structural elements is imperative for proper connection design. However, the design of the existing connections and development of novel connections require knowledge of the range and distribution of forces a connection may experience over its lifetime, irrespective of parametric variations. In this part, the results for maximum and minimum axial forces for the skewed cross-frame members under the Fatigue–I envelope forces are shown in Table 7. Figures 20 and 21 illustrate examples of the maximum (tensile) and minimum (compressive) forces, respectively, experienced by skewed end cross-frame members in Bridge 23 under Fatigue-1 envelope loading.

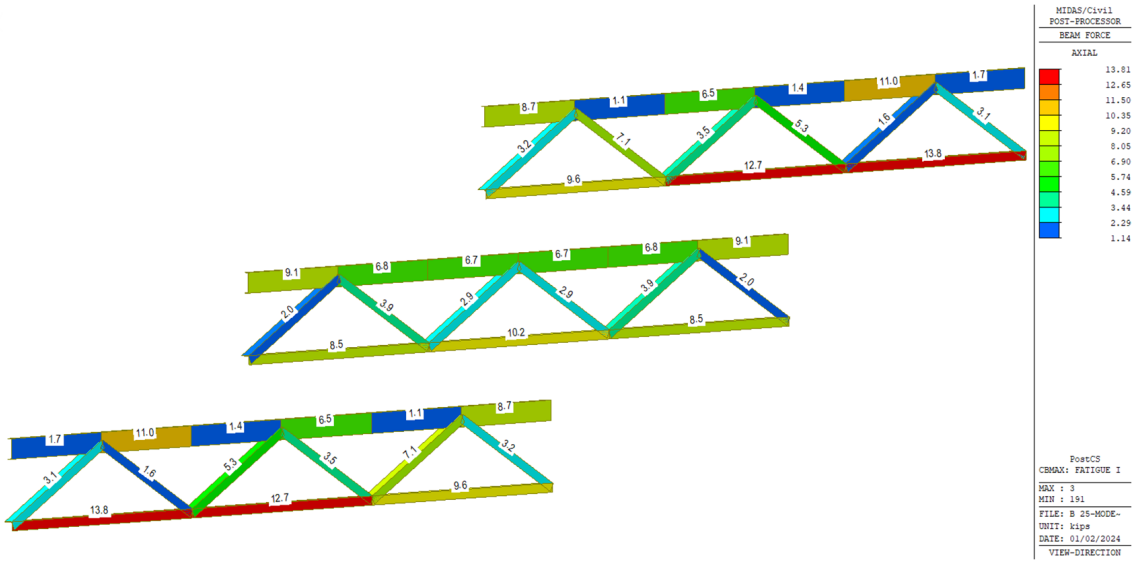


Figure 20. Maximum tensile forces in skewed end cross-frame members of Bridge 23 under Fatigue–I envelope loading conditions (measured in ksi).

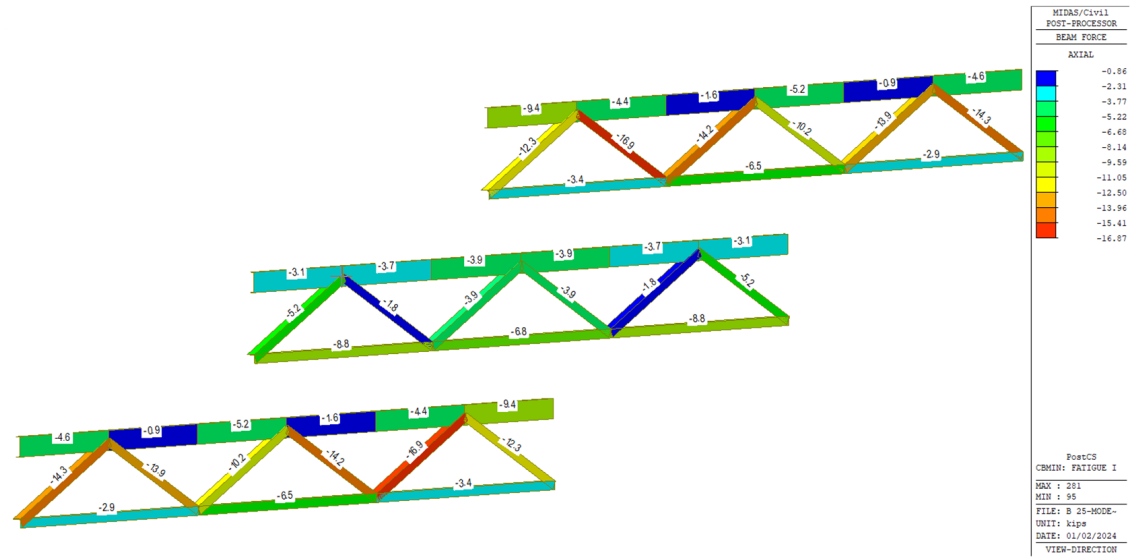


Figure 21. Maximum compressive forces in skewed end cross-frame members of Bridge 23 under Fatigue–I envelope loading conditions (measured in ksi).

Table 7. Skewed cross-frame members' axial forces for Fatigue–I envelope (measured in ksi).

Bridge Number	Top Chord Force (ksi)		Diagonal Elements Force (ksi)		Bottom Chord Force (ksi)	
	Min	Max	Min	Max	Min	Max
1	−7.6	14.0	−15.8	4.7	−8.8	10.5
2	−8.9	10.3	−19.5	8.3	−11.5	18.0
3	−4.5	16.2	−8.0	4.9	−4.4	26.2
4	−6.8	15.9	−6.0	5.6	−17.4	14.5
5	−9.5	19.6	−5.7	5.7	−10.7	12.4
6	−8.5	16.2	−6.0	6.1	−17.4	25.6
7	−18.6	12.7	−12.5	9.1	−32.1	36.5
8	−4.8	17.1	−3.8	3.8	−11.4	13.9
9	−6.6	12.6	−20.3	6.3	−25.1	36.1
10	−6.5	7.7	−10.3	9.8	−13.7	21.1
11	−11.7	20.8	−12.8	12.2	−22.3	27.5
12	−7.1	16.1	−20.2	4.9	−9.2	16.1
13	−6.2	18.8	−9.0	6.6	−8.9	13.2
14	−7.6	14.2	−26.1	7.8	−9.4	20.9
15	−4.6	8.5	−24.5	7.4	−18.1	23.4
16	−6.3	17.0	−15.3	2.9	−5.2	12.4
17	−5.2	9.2	−14.7	5.1	−7.1	8.8
18	−6.0	11.5	−12.6	4.0	−8.8	9.9
19	−8.3	13.4	−13.8	5.5	−2.9	10.9
20	−5.8	11.9	−11.7	3.0	−2.1	7.2
21	−7.0	11.0	−14.2	5.2	−11.2	12.0
22	−5.1	8.9	−15.5	4.1	−4.3	8.8
23	−9.4	11.0	−16.9	7.1	−8.8	13.8
24	−13.0	10.0	−11.0	3.6	−8.9	12.5
25	−9.7	10.4	−11.3	4.6	−8.2	9.0
26	−7.7	9.7	−12.4	10.3	−13.2	16.9

The histograms provided in Figures 22–27 represent the distribution of the maximum tensile and compressive axial force due to Fatigue–I loading in cross-frame elements collected from the analysis of 26 representative skew bridges located in Florida. The *x*-axis of the histogram represents ranges of axial force in kips (kilo-pound force), divided into intervals, while the *y*-axis represents the number of bridges that fall within each axial force range. Positive and negative force values represent tension and compression in the element, respectively. The forces shown are factored forces. In Figure 22, the maximum tensile internal force in top chord elements of cross-frames is between 7.7 and 20.8 kips, with the most common value for 27% of the bridges being between 9.9 and 12.1 kips, while the average axial force value is 13.3 kips. The histogram is also notable for its relatively narrow range. The maximum internal force in all 26 bridges is within 10 kips of the average value. This suggests that the maximum internal force in top chord elements of the cross-frames is relatively consistent across the selected Florida bridges.

Furthermore, the histogram in Figure 23 illustrates the distribution of compressive axial forces in cross-frame top chord elements of the 26 Florida bridges under Fatigue–I loading. Most bridges fall into the range of (−6.9, −4.5) kips, indicating this as the most common interval for axial compressive forces. The data suggest a higher frequency of lower-magnitude compressive forces, with the number of bridges generally decreasing as the force interval magnitudes increase.

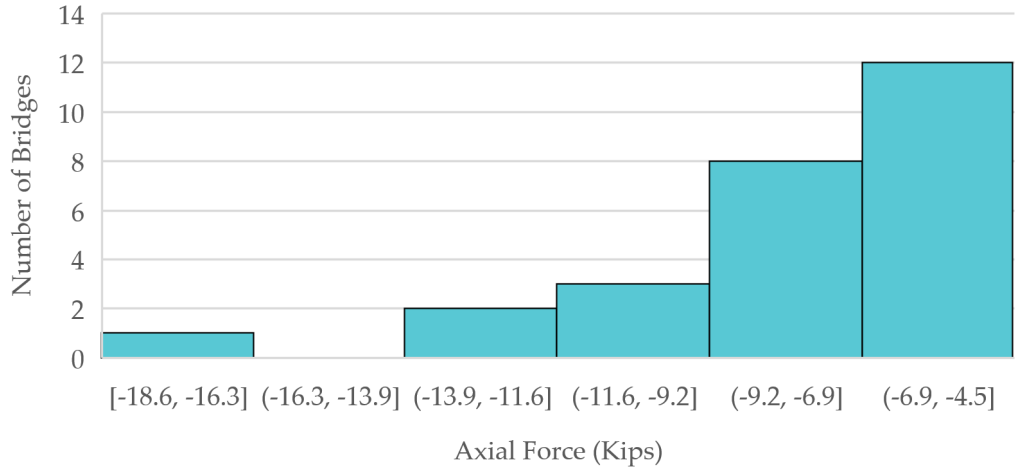


Figure 22. Tensile axial force distribution in top chord elements for Fatigue–I envelope (kips).

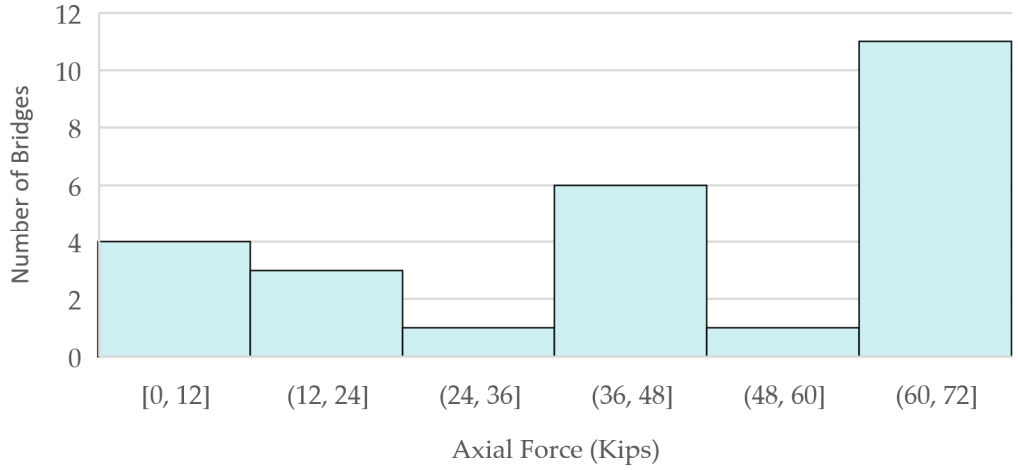


Figure 23. Compressive axial force distribution in top chord elements for Fatigue–I envelope (kips).

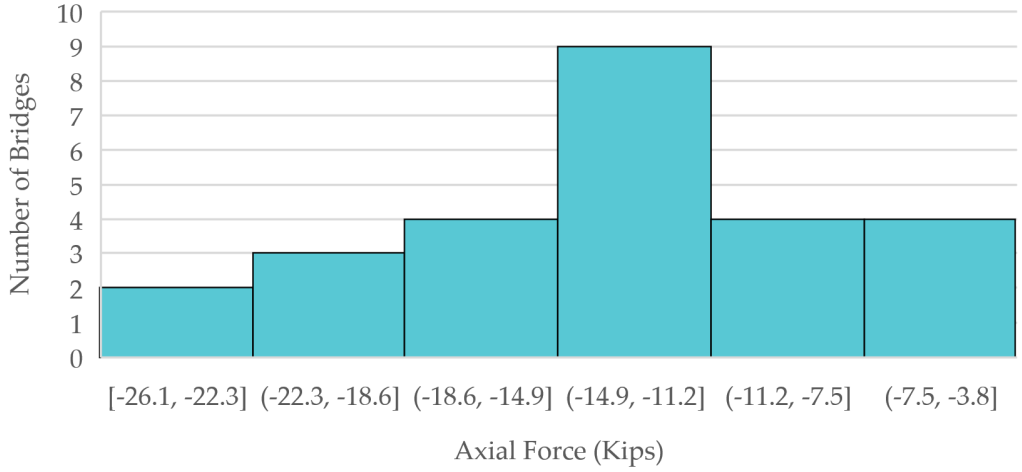


Figure 24. Tensile axial force distribution in diagonal elements for Fatigue–I envelope (kips).

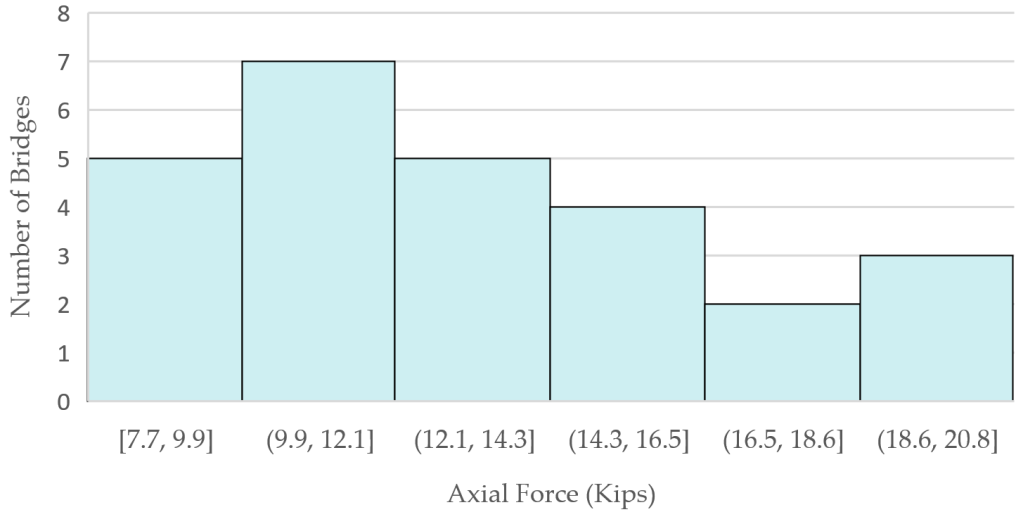


Figure 25. Compressive axial force distribution in diagonal elements for Fatigue–I envelope (kips).

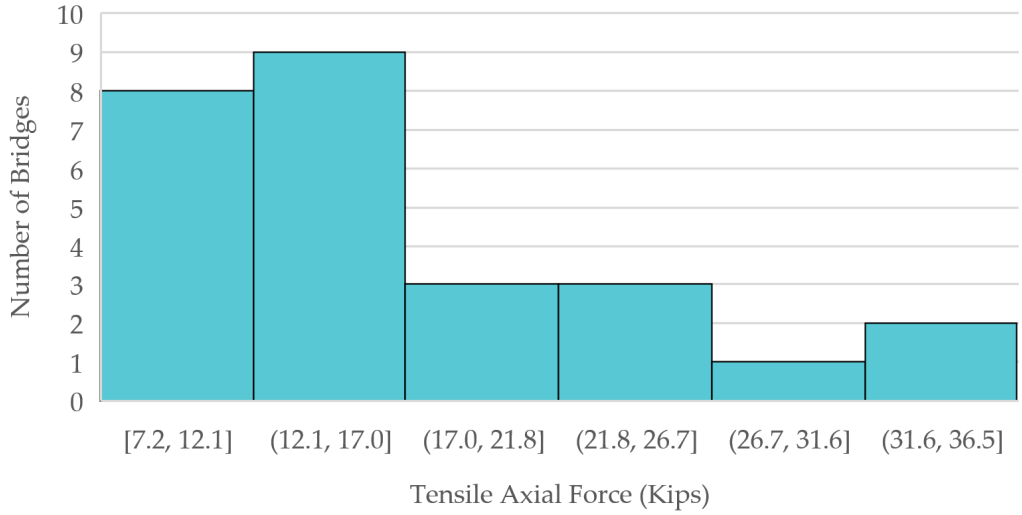


Figure 26. Tensile axial force distribution in bottom chord elements for Fatigue–I envelope (kips).

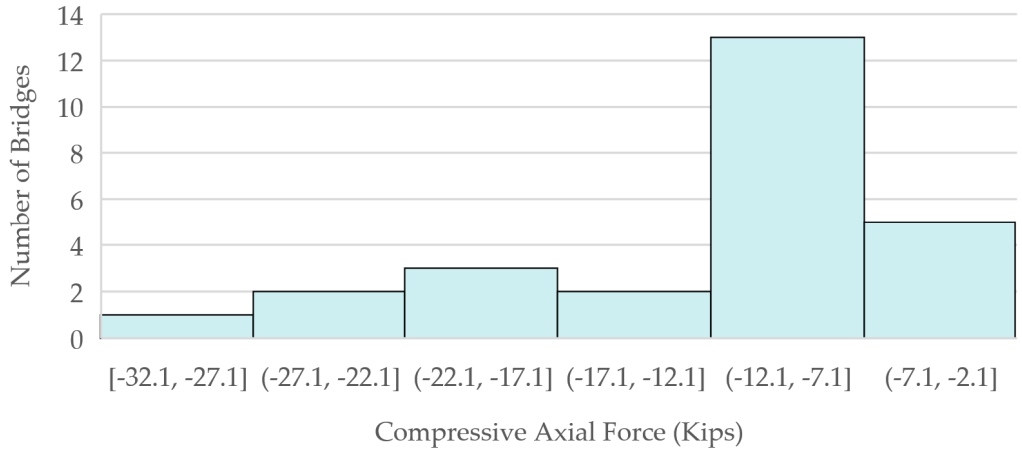


Figure 27. Compressive axial force distribution in bottom chord elements for Fatigue–I envelope (kips).

Similar observations can be made from Figures 24 and 25 showing tensile (maximum) and compressive (minimum) forces from Fatigue-1 loading in diagonal elements, and from Figures 26 and 27 for bottom chords of the end cross-frames.

3.3. Fatigue Consideration in Skewed Connections

Fatigue is also a significant concern for connection components, particularly in skewed bridges. As previously noted, the two common types of skewed connections in such bridges are the Half-Round Bearing Stiffener (HRBS) and Bent Plates. The fatigue category for the connection itself, mainly for the HRBS, has not been defined. There is no detail in Table 4.5 of the AWS D1.1/D1.1M [38] or Table 6.6.1.2.3-1 of the AASHTO LRFD [2] that could represent the HRBS connection. Consequently, this section aims only to identify potential fatigue-prone zones to predict the likely locations of fatigue-crack initiation within these connections, and stress risers that may affect the fatigue performance of the connection.

The FE analysis was carried out to determine the stress distribution within the Half-Round Bearing Stiffener (HRBS) and bent plate connection of a selected bridge. Bridge 9 with the largest steel girders was selected for this analysis. For the loading, the highest range of the Fatigue–I envelope forces at the end cross-frames was selected. Hence, the results will also compare these two connection types in relation to fatigue stresses and stress concentration. The modeling focused on the cross-frame connection to a steel girder, including nearby structural components such as the concrete deck, skewed pier, end cross-frame members forces, and support bearings. Finer mesh (with approximately 1-inch size meshes) and more representative types of elements (solid vs. plate) were used for this detailed analysis when compared to the analysis of bridges reported earlier. Boundary conditions reflected the restraint provided by the composite deck and support elements. The steel I-girder utilized ASTM A 709 GRADE 50 structural steel. The FE model included discrete components interconnected through rigid weld connections. For the HRBS connection, two cases were modeled, one with a stiffener plate welded to the girder flanges and the other with unwelded stiffener plates. MIDAS FEA NX 2024 (v1.1) software facilitated the use of Solid 3D elements, employing a hybrid mesh system to model complex geometries effectively. Critical load combination using the highest envelope forces ensured conservative yet practical load effects. The principal stresses from this refined analysis are shown in Table 8. The results demonstrate that for the HRBS connection, welding the stiffener plate to the girder flanges reduces the stress concentration in the HRBS and stiffener plate. Also, as expected, the use of HRBS improves the stress distribution by eliminating the bent plate, which is the point of concern for stress concentration. Fatigue-prone zones and potential crack-initiation locations are highlighted in this table, providing insights into the fatigue performance of the connections.

Table 8. SCR and positions in HRBS, stiffener plate, and girder from Fatigue I for Bridge 9.

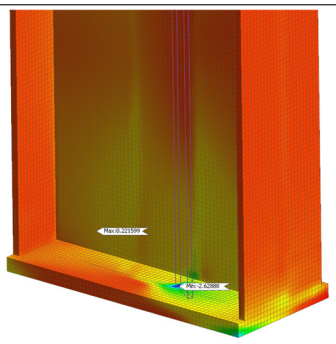
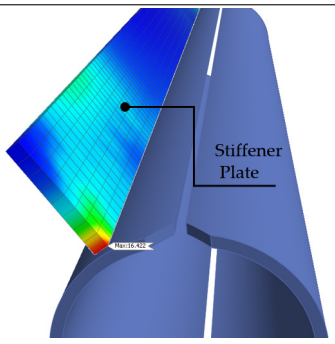
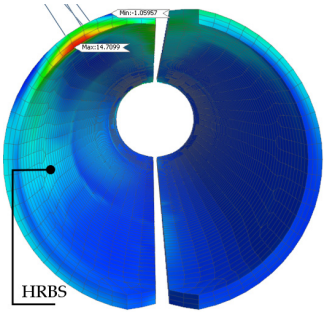
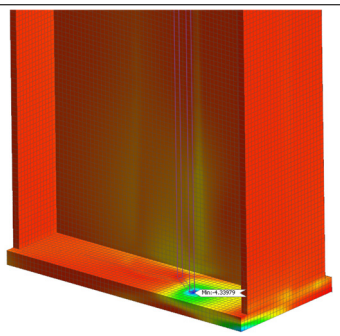
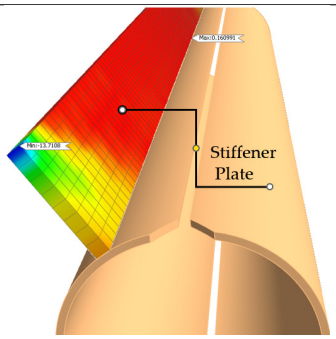
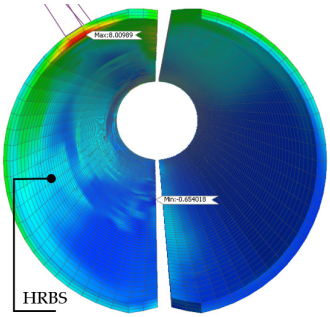
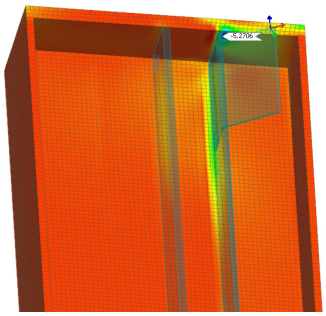
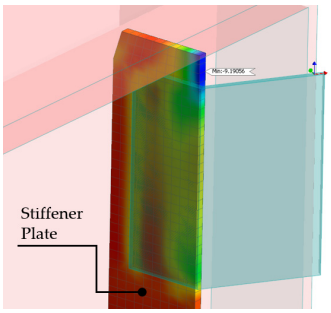
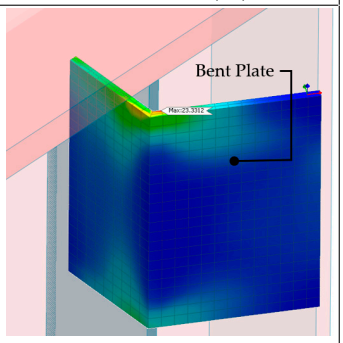
Weld Condition	Skewed Connection Type	Maximum Principal Stress Concentration Range and Position in Steel I-Girder	Maximum Principal Stress Concentration Range and Position in Stiffener Plate	Maximum Principal Stress Concentration Range and Position in Skewed Connection
Unwelded	Half-Round Bearing Stiffener	 Max SCR = 2.62 (ksi)	 Max SCR = 16.42 (ksi)	 Max SCR = 14.71 (ksi)

Table 8. *Cont.*

Weld Condition	Skewed Connection Type	Maximum Principal Stress Concentration Range and Position in Steel I-Girder	Maximum Principal Stress Concentration Range and Position in Stiffener Plate	Maximum Principal Stress Concentration Range and Position in Skewed Connection
Welded	Half-Round Bearing Stiffener	 Max SCR = 4.33 (ksi)	 Max SCR = 13.71 (ksi)	 Max SCR = 8.00 (ksi)
Welded	Bent Plate	 Max SCR = 5.27 (ksi)	 Max SCR = 9.19 (ksi)	 Max SCR = 23.33 (ksi)

4. Conclusions

The study outlined in this paper relates to the fatigue behavior of the tension flange over intermediate supports in skewed continuous steel I-girder bridges. A wide range of bridge geometries representing skew bridges in the State of Florida was included in this study. Support skew generally complicates the load path, secondary stresses, and differential girder movements. End cross-frames over piers and abutments normally connect to the girders at an angle matching the skew to facilitate the force transfer. The literature review covered cross-frame configuration, effectiveness, and connection types like bent plates or half-round stiffeners. The following conclusions can be made from this study:

- Finite element analyses of 26 bridges representing the range of geometries of skew bridges in the State of Florida were utilized to quantify flange fatigue stress ranges and axial forces in the cross-frame members for fatigue assessment.
- A preliminary analysis helped to identify the appropriate modeling details. This included the use of plate FE elements for the deck and girders, and beam elements for cross-frame members. Also, the analysis showed that the effect of modeling the substructure is negligible when the neoprene bearings are included.
- The maximum top-flange fatigue stress range at the intermediate supports under fatigue truck loading was found to be 3.63 ksi. This condition is shown in Figure 3 in relation to the weld between the stiffener plate and the girder flange.
- The calculated factored fatigue stress ranges are well below the fatigue threshold of 10 ksi for AASHTO Category C or 12 ksi for Category C' normally associated with such connections, shown in Figure 3. Therefore, fatigue is not likely to be a concern in the flanges themselves.
- Forces in the skewed end cross-frame members were also presented, providing data for future studies.

- A refined FE model of a skew connection of an end cross-frame to the steel girder was constructed to investigate the connection under fatigue loading. The maximum fatigue envelope force ranges were applied on this connection to study the stress concentration range and location of stress risers. The results show that a Half-Round Bearing Stiffener (HRBS) improves the stress distribution, especially when the stiffener plate is welded to the girder flanges. The stress concentration range calculated in the girder flange is around 18 to 50 percent lower for the HRBS connection compared to the bent plate connection for the welded and unwelded conditions, respectively. For the connection components, the maximum stress concentration range for the bent plate is 23.33 ksi, which is significantly higher than the maximum stress concentration range of 16.42 ksi for the stiffener plate connected to HRBS.

This study has addressed the knowledge gap on fatigue concerns for the top flange of the steel girders over the intermediate supports for skewed bridges. It has also generated a wealth of information for further investigations into the fatigue behavior of skew connections and the design and detailing of new types of connections addressing the shortcomings of the currently available details. A limited connection refined modeling has pointed to the positive effects of using HRBS details. Future study can focus on a broader parametric study to make the results more inclusive regarding a larger population of bridges, connection detail improvements, multi-scale refined FE modeling to facilitate the connection design, and if needed, experimental fatigue and load-testing planning for verification purposes. Additionally, alongside fatigue testing, conducting corrosion evaluations on these connections is crucial, particularly in humid or marine environments where corrosion detrimentally impacts structural integrity [24].

Author Contributions: Conceptualization, D.T., S.S.K.D., A.M. and T.A.H.; methodology, D.T., S.S.K.D., A.M. and T.A.H.; software, D.T., S.S.K.D. and A.M.; validation, D.T., S.S.K.D. and A.M.; formal analysis, D.T., S.S.K.D., A.M. and T.A.H.; investigation, D.T., S.S.K.D., A.M. and T.A.H.; resources, D.T., S.S.K.D. and A.M.; data curation, D.T.; writing—original draft preparation, D.T., S.S.K.D. and A.M.; writing—review and editing, D.T., S.S.K.D., A.M. and T.A.H.; visualization, D.T., S.S.K.D. and A.M.; supervision, A.M. and T.A.H.; project administration, A.M. and T.A.H.; funding acquisition, A.M. and T.A.H. All authors have read and agreed to the published version of the manuscript.

Funding: This research was funded by Florida Department of Transportation (FDOT), contract number BED65—Project ID. 4407441B201.

Data Availability Statement: The data presented in this study are available on request from the corresponding author.

Acknowledgments: This project for which this study was performed is supported by the Florida Department of Transportation (FDOT). The opinions, findings, and conclusions expressed in this publication are those of the author(s) and not necessarily those of the Florida Department of Transportation or the U.S. Department of Transportation.

Conflicts of Interest: The authors declare that they have no known competing financial interests or personal relationships that could have appeared to influence the work reported in this paper.

References

1. U.S. Department of Transportation; Federal Highway Administration (FHWA). *National Bridge Inventory*; Federal Highway Administration (FHWA): Washington, DC, USA, 2022.
2. AASHTO. *AASHTO LRFD Bridge Design Specifications*, 9th ed.; American Association of State Highway and Transportation Officials: Washington, DC, USA, 2020.
3. Menassa, C.; Mabsout, M.; Tarhini, K.; Frederick, G. Influence of skew angle on reinforced concrete slab bridges. *J. Bridge Eng.* **2007**, *12*, 205–214. [CrossRef]
4. Bishara, A.G.; Liu, M.C.; El-Ali, N.D. Wheel load distribution on simply supported skew I-beam composite bridges. *J. Struct. Eng.* **1993**, *119*, 399–419. [CrossRef]
5. Rajagopalan, N. *Bridge Superstructure*; Alpha Science Int'l Ltd.: Oxford, UK, 2006.
6. Wang, L. *Cross-Frame and Diaphragm Behavior for Steel Bridges with Skewed Supports*; University of Houston: Houston, TX, USA, 2002.

7. Connor, R.J.; Lloyd, J.B. *Maintenance Actions to Address Fatigue Cracking in Steel Bridge Structures*; NCHRP Project; Transportation Research Board: Washington, DC, USA, 2017.
8. Gunes, B.; Ilki, A.; Oztorun, N.K. Determination of Monitoring Parameters for Fatigue Behavior of Steel-Concrete Composite Bridge Girders with Welded Full Depth Transverse Stiffeners. *Sustainability* **2020**, *12*, 283. [CrossRef]
9. Berglund, E.M.; Schultz, A.E. Girder differential deflection and distortion-induced fatigue in skewed steel bridges. *J. Bridge Eng.* **2006**, *11*, 169–177. [CrossRef]
10. Connor, R.J.; Fisher, J.W. Identifying effective and ineffective retrofits for distortion fatigue cracking in steel bridges using field instrumentation. *J. Bridge Eng.* **2006**, *11*, 745–752. [CrossRef]
11. Tabiatnejad, B.; Siddiqua, S.; Siemens, G. Impact of pore fluid salinity on the mechanical behavior of unsaturated bentonite–sand mixture. *Environ. Earth Sci.* **2016**, *75*, 1434. [CrossRef]
12. Hartman, A.S.; Hassel, H.L.; Adams, C.A.; Bennett, C.R.; Matamoros, A.B.; Rolfe, S.T. Effects of cross-frame placement and skew on distortion-induced fatigue in steel bridges. *Transp. Res. Rec.* **2010**, *2200*, 62–68. [CrossRef]
13. McConnell, J.R.; Almoosi, Y.S. Field Evaluation of Fatigue Stresses in a Modern Highly Skewed Steel I-Girder Bridge. *J. Bridge Eng.* **2022**, *27*, 4022005. [CrossRef]
14. Tedesco, J.; Stallings, J.; Tow, D. Finite element method analysis of bridge girder-diaphragm interaction. *Comput. Struct.* **1995**, *56*, 461–473. [CrossRef]
15. Dong, Z.-Q.; Li, G.; Li, H.-N. Dynamic tests of the collapse-prevention performance of a low-ductility low-rise steel concentrically braced frame. *Eng. Struct.* **2021**, *240*, 112420. [CrossRef]
16. Schaefer, A.L. Crossframe Analysis of Highly-Skewed and Curved Steel I-Girder Bridges. Ph.D. Thesis, University of Colorado at Denver, Denver, CO, USA, 2012.
17. Quadrato, C.; Wang, W.; Battistini, A.; Wahr, A.; Helwig, T.; Frank, K.; Engelhardt, M. *Cross-Frame Connection Details for Skewed Steel Bridges*; University of Texas at Austin, Center for Transportation Research: Austin, TX, USA, 2010.
18. Astaneh-Asl, A.; Bolt, B.; McMullin, K.M.; Donikian, R.; Modjtahedi, D.; Cho, S. *Seismic Performance of Steel Bridges during the 1994 Northridge Earthquake*; University of California at Berkeley: Berkeley, CA, USA, 1994.
19. Bruneau, M.; Wilson, J.C.; Tremblay, R. Performance of steel bridges during the 1995 Hyogo-ken Nanbu (Kobe, Japan) earthquake. *Can. J. Civ. Eng.* **1996**, *23*, 678–713. [CrossRef]
20. Ballantyne, D.; Borcherdt, R.D.; Buckle, I.G.; O'Rourke, T.D.; Schiff, A.J. *The Hanshin-Awaji Earthquake of January 17, 1995: Performance of Lifelines*; National Center for Earthquake Engineering Research: Taipei, Taiwan, 1995.
21. Carden, L.; Itani, A.; Buckle, I. An Experimental Study into the Distribution of Earthquake Forces in Steel Plate Girder Bridges. In Proceedings of the Pacific Conference on Earthquake Engineering, Christchurch, New Zealand, 13–15 February 2003.
22. Kloiber, L.A. *Orthogonal and Skewed Shear Connections—Design and Detailing Requirements*; American Institute of Steel Construction (AISC): Chicago, IL, USA, 2004.
23. Mehrabi, A.; Tabiatnejad, D.; Dolati, S.S.K. Connection Systems and Methods for Skewed Frames. U.S. Patents 11746484, 5 September 2023.
24. Mehrabi, A.; Farhangdoust, S.; Dolati, S.S.K.; Tabiatnejad, D.; Lee, S.J.; Garber, D. *Epoxy Dowel Pile Splice Evaluation*; Research Center, Florida Department of Transportation: Tallahassee, FL, USA, 2022.
25. *G12.1—Guidelines for Design Constructability*; AASHTO/NSBA Steel Bridge Collaboration: Chicago, IL, USA, 2003.
26. Battistini, A.D.; Wang, W.; Helwig, T.A.; Engelhardt, M.D.; Frank, K.H. Stiffness behavior of cross frames in steel bridge systems. *J. Bridge Eng.* **2016**, *21*, 4016024. [CrossRef]
27. Quadrato, C.; Battistini, A.; Helwig, T.; Engelhardt, M.; Frank, K. Increasing Girder Elastic Buckling Strength Using Split Pipe Bearing Stiffeners. *J. Bridge Eng.* **2014**, *19*, 4013017. [CrossRef]
28. *mBrace3D*, 2.0; Nessos Information Technologies SA: Athens, Greece, 2023.
29. MIDAS. *MIDAS Civil (Software)*, MIDAS IT: Seongnam, Republic of Korea, 2024.
30. Reichenbach, M.; White, J.; Park, S.; Zecchin, E.; Moore, M.; Liu, Y.; Liang, C.; Kövesdi, B.; Helwig, T.; Engelhardt, M. *Proposed Modification to AASHTO Cross-Frame Analysis and Design*; National Academies of Sciences, Engineering, and Medicine: Washington, DC, USA, 2021.
31. Gull, J.H.; Azizinamini, A.; Helwig, T.A. Comparison of detailing methods for straight skewed steel I-girder bridges. *J. Constr. Steel Res.* **2017**, *136*, 24–34. [CrossRef]
32. Horas, C.S.; De Jesus, A.M.; Calçada, R. Efficient progressive global-local fatigue assessment methodology for existing metallic railway bridges. *J. Constr. Steel Res.* **2022**, *196*, 107431. [CrossRef]
33. Horas, C.S.; De Jesus, A.M.; Ribeiro, D.; Calçada, R. Efficient multiscale methodology for local stress analysis of metallic railway bridges based on modal superposition principles. *Eng. Fail. Anal.* **2022**, *138*, 106391. [CrossRef]
34. De Jesus Abílio, M.; Rui, C. Efficient computational approach for fatigue assessment of riveted connections. *J. Constr. Steel Res.* **2019**, *153*, 1–18.
35. Albuquerque, C.; Silva, A.L.; de Jesus, A.M.; Calçada, R. An efficient methodology for fatigue damage assessment of bridge details using modal superposition of stress intensity factors. *Int. J. Fatigue* **2015**, *81*, 61–77. [CrossRef]
36. Correia, J.A.; da Silva, A.L.; Xin, H.; Lesiuk, G.; Zhu, S.-P.; de Jesus, A.M.; Fernandes, A.A. Fatigue performance prediction of S235 base steel plates in the riveted connections. In *Structures*; Elsevier: Amsterdam, The Netherlands, 2021; pp. 745–755.

37. Aygül, M.; Al-Emrani, M.; Barsoum, Z.; Leander, J. Investigation of distortion-induced fatigue cracked welded details using 3D crack propagation analysis. *Int. J. Fatigue* **2014**, *64*, 54–66. [CrossRef]
38. *AWS D1. 1/D1. 1M*; Structural Welding Code Steel. American Welding Society: Miami, FL, USA, 2020.

Disclaimer/Publisher's Note: The statements, opinions and data contained in all publications are solely those of the individual author(s) and contributor(s) and not of MDPI and/or the editor(s). MDPI and/or the editor(s) disclaim responsibility for any injury to people or property resulting from any ideas, methods, instructions or products referred to in the content.